PHYSICAL REVIEW B **88**, 041105(R) (2013)

Suppression of Brewster delocalization anomalies in an alternating isotropic-birefringent random layered medium

T. M. Jordan

School of Biological Sciences, Woodland Road, University of Bristol, Bristol BS8 1UG, United Kingdom and Bristol Centre for Complexity Sciences, Queens Building, University Walk, University of Bristol, Bristol BS8 1TR, United Kingdom

J. C. Partridge and N. W. Roberts*

School of Biological Sciences, Woodland Road, University of Bristol, Bristol BS8 1UG, United Kingdom

(Received 3 April 2013; published 11 July 2013)

We investigate the polarization dependence of localization length in alternating isotropic-birefringent stacks with uncorrelated thickness disorder. The birefringent layers can be positive uniaxial, negative uniaxial, or a mixture of both. Stacks which contain a mixture are shown to suppress the Brewster delocalization anomalies and, over all incident angles, exhibit p-polarization localization length maxima that are of similar magnitude to normal incidence. Furthermore, we propose a parameter set that enables the p-polarization localization length to monotonically decrease with angle of incidence. This investigation was inspired by weakly polarizing mirrors on the sides of silvery fish and provides a generic means to produce polarization-insensitive, broadband reflections from a random, all-dielectric layered medium.

DOI: 10.1103/PhysRevB.88.041105 PACS number(s): 42.25.Dd, 42.25.Ja, 42.25.Lc, 87.19.lt

Localization is a concept that explains how quantum wave functions and classical electromagnetic waves become spatially confined due to disorder.[1,2] It arises entirely due to multiple scattering and interference,[3] and is most strongly apparent in 1-dimensional (1D) random layered media. In these 1D "stack" systems, all scalar stationary quantum wave states are proven to localize.[4,5] However, exceptions to localization occur for the stationary states of vectorial electromagnetic waves referred to as "Brewster delocalization anomalies."[6–12] This effect corresponds to the pronounced suppression, and in some special circumstances complete inhibition, of localization at oblique incidence for p-polarized light. It is a highly robust behavior present in both strongly disordered stacks (e.g., where there is uncorrelated layer thicknesses[6–8]), and weakly disordered stacks (e.g., where there is uniform disorder about a mean thickness[11]).

Broadband, mirror-like reflections from a random dielectric medium are a physical realization of the localization of electromagnetic waves.[13] The principles of localization have subsequently been used to inform the design of high-performance broadband mirrors, which have a broader reflection band than periodic systems with the same refractive indices (e.g., Refs. 14 and 15). If a stack system could be devised that was effective at localizing both s- and p-polarized light over all angles of incidence, it would provide a means to produce polarization-insensitive, broadband reflections. This is a highly desirable optical property and existing nonpolarizing dielectric mirrors have applications that include waveguides and thermoelectric devices.[16]

In this Rapid Communication, we demonstrate that stacks which include both positive and negative uniaxial birefringent layers can suppress the Brewster delocalization anomalies, and subsequently provide a mechanism to produce broadband, polarization-insensitive reflections. Our model system was motivated by our previous analysis of the nonpolarizing reflections from the birefringent guanine and isotropic cytoplasm multilayer structure found in some species of silvery fish.[17] While the investigation of animal photonics continues to be of great inspiration for the design of practical optical devices,[18–20] our study aims to illustrate how such biological optical structures can also inspire systems of interest to theoretical physics.

The general model of our stack system consists of alternating isotropic and uniaxial birefringent layers embedded in an isotropic medium (Fig. 1). The birefringent layers are a mixture of randomly ordered negative and positive types, with refractive index vectors

$$\mathbf{n}_- = (n_a, n_a, n_b), \quad \mathbf{n}_+ = (n_b, n_b, n_a). \tag{1}$$

The isotropic layers and external media both have refractive index n_0. It is assumed that $n_a \geqslant n_b \geqslant n_0$. This criterion ensures that light is able to access all angles of incidence at each isotropic-birefringent interface in the stack, and consequently that critical angle screening does not occur. This stack mimics the guanine-cytoplasm structure in fish skin where there are two different types of birefringent guanine crystal present with isotropic cytoplasm gaps.[17] However, this stack has been simplified from the biological system to be rotationally symmetric about the z axis (the direction of stacking), which is a sufficient condition for the s- and p-polarization modes to be separable.

The general matrix formalism for anisotropic layered media[21,22] enables us to calculate numerically the exact transmission of the stacks. The 2×2 transfer matrix for each polarization mode, M, is of the form

$$M_i = \begin{bmatrix} \cos(\delta_i) & -\frac{i}{\beta_i}\sin(\delta_i) \\ -i\beta_i \sin(\delta_i) & \cos(\delta_i) \end{bmatrix}, \quad M = \prod_i M_i, \tag{2}$$

where β_i are transverse refractive indices defined by

$$\beta_i = \begin{cases} \frac{n_{i,x} n_{i,z}}{\sqrt{n_{i,z}^2 - n_0^2 \sin^2(\theta)}} & p\text{-polarization}, \\ \sqrt{n_{i,y}^2 - n_0^2 \sin^2(\theta)} & s\text{-polarization}, \end{cases} \tag{3}$$

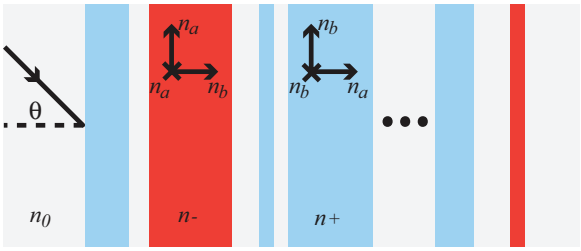

FIG. 1. (Color online) The system geometry. The red and blue regions represent negative and positive uniaxial layers respectively, while the gray regions represent the isotropic layers and external media. The orientation of the principle axes for the birefringent layers is shown, with the y coordinate into the page and the z coordinate aligned with stacking direction. θ denotes the angle of incidence.

and δ_i are phase thicknesses defined by

$$\delta_i = \begin{cases} \left(\frac{2\pi}{\lambda}\right) a_i n_{i,x} \sqrt{1 - \left(\frac{n_0 \sin(\theta)}{n_{i,z}}\right)^2} & p\text{-polarization}, \\ \left(\frac{2\pi}{\lambda}\right) a_i n_{i,y} \sqrt{1 - \left(\frac{n_0 \sin(\theta)}{n_{i,y}}\right)^2} & s\text{-polarization}, \end{cases} \tag{4}$$

with i indexing each layer, x, y, z indexing each Cartesian coordinate direction, λ the wavelength, a the layer thickness, and θ the angle of incidence. It is assumed that the s-polarization is aligned with the y direction. The stack transmission, $T_{s,p}$, is then calculated using standard formulas.[22] Equations (2)–(4) generalize to birefringent-birefringent interfaces and biaxial layers where the principle axes and polarization components are aligned with the Cartesian coordinate directions.

To calculate the localization length, $\xi_{s,p}$, we use the definition[23]

$$\xi_{s,p} = -\left\langle \frac{2L}{\ln T_{s,p}} \right\rangle, \tag{5}$$

where L is the system length and $\langle\ \rangle$ denotes ensemble average. The localization length can also be defined as a non-self-averaging quantity for an infinite stack length.[24] Equation (5) is valid for systems where the number of layers in the stacks is $\ll \xi_{s,p}$ and provides a more practical means to numerically compute $\xi_{s,p}$ by using log-linear regression of Eq. (5) and sampling over a random set of stack configurations.

In the guanine-cytoplasm multilayer of fish skin the layer thicknesses are assumed to be uniformly distributed about a mean value.[17] However, here we chose to adapt an existing analytical model for strong uncorrelated thickness disorder.[6–8] This has the advantage of enabling us to make the clearest connection between the localization length and reflection coefficients of the individual scattering layers. This model is a weak scattering limit of a general formulation for the transmission of waves through one-dimensional systems[8] and assumes that the reflection coefficients are $\ll 1$. The layer thicknesses are sampled from an exponential probability distribution,

$$P(a) = \exp\left(\frac{a}{a_0}\right), \tag{6}$$

where a_0 is the mean layer thickness. The wavelength-independent expression for $\xi_{s,p}$ (in units of a_0) is given by[7,8]

$$\frac{\xi_{s,p}}{a_0} = \frac{2}{r_{s,p}^2}, \tag{7}$$

where $r_{s,p}^2$ is the average interfacial intensity reflection coefficient in the system. As this formula is valid for stacks with an arbitrary refractive index distribution, it subsequently can be applied to stacks with birefringent layers where the polarization modes are separable. For our alternating isotropic-birefringent stack,

$$r_{s,p}^2 = (1 - f) r_{s+,p+}^2 + f r_{s-,p-}^2, \tag{8}$$

where $0 \leqslant f \leqslant 1$ is the mixing ratio of negative to positive birefringent layer types. The intensity reflection coefficients are obtained by substituting the refractive index vectors, (1), into the generalized isotropic-birefringent Fresnel relations:[22]

$$r_{s_{+,-}}^2 = \left(\frac{n_0 \cos(\theta) - \sqrt{n_{i,y}^2 - n_0^2 \sin^2\theta}}{n_0 \cos(\theta) + \sqrt{n_{i,y}^2 - n_0^2 \sin^2\theta}} \right)^2, \tag{9}$$

$$r_{p_{+,-}}^2 = \left(\frac{n_0 n_{i,x} n_{i,z} \cos(\theta) - n_0^2 \sqrt{n_{i,z}^2 - n_0^2 \sin^2(\theta)}}{n_0 n_{i,x} n_{i,z} \cos(\theta) + n_0^2 \sqrt{n_{i,z}^2 - n_0^2 \sin^2(\theta)}} \right)^2. \tag{10}$$

The angular dependence of $\xi_{s,p}$ for binary isotropic-birefringent stacks (corresponding to isotropic-positive uniaxial stacks for $f = 0$ and isotropic-negative uniaxial stacks for $f = 1$) is shown in Fig. 2(a) for $n_a = 1.83$, $n_b = 1.46$, $n_0 = 1.33$. It is clear that there is a very close agreement between the numerical transfer matrix simulations and the weak scattering approximation over all angles of incidence. The localization lengths of the stack system can therefore be well understood from the properties of the s and p reflection coefficients of the respective isotropic-birefringent interfaces [(9), (10), and Fig. 3(a)]. The divergence in $\xi_{s,p}$ occurs at the generalized anisotropic Brewster angle

$$\tan(\theta_B) = \left(\frac{n_{i,z}}{n_0}\right) \sqrt{\left(\frac{n_0^2 - n_{i,x}^2}{n_0^2 - n_{i,z}^2}\right)} \tag{11}$$

(Ref. 25), where the interfacial reflection coefficients for p-polarized light are zero and $T_{s,p} = 1$. In this scenario, the necessary scattering and interference required for localization to occur is completely inhibited. Both curves in Fig. 2(a) are qualitatively similar to isotropic binary structures,[6,7,10,11] with both nonmonotonic behavior and fully divergent Brewster anomalies for ξ_p, and monotonically decreasing ξ_s with angle of incidence. However, the freedom in the shifting of the angular position of θ_B from Eq. (11) is far more pronounced than isotropic-isotropic interfaces where $\tan(\theta_B) = (n_{i,z}/n_0)$ with $n_{i,z} = n_{i,x}$. It follows from (11) that in the most general form of our model, θ_B can be anywhere between 0° and 90° with $\theta_B > \tan^{-1}(n_{i,z}/n_0)$ for the isotropic-negative uniaxial interfaces and $\theta_B < \tan^{-1}(n_{i,z}/n_0)$ for the isotropic-positive uniaxial interfaces. The set refractive index values follow the ordinary and extraordinary indices of the biogenic guanine crystals and cytoplasm in fish skin[26] and have $\theta_B \approx 33°, 67°$ for $f = 0, 1$ mixing ratios respectively.

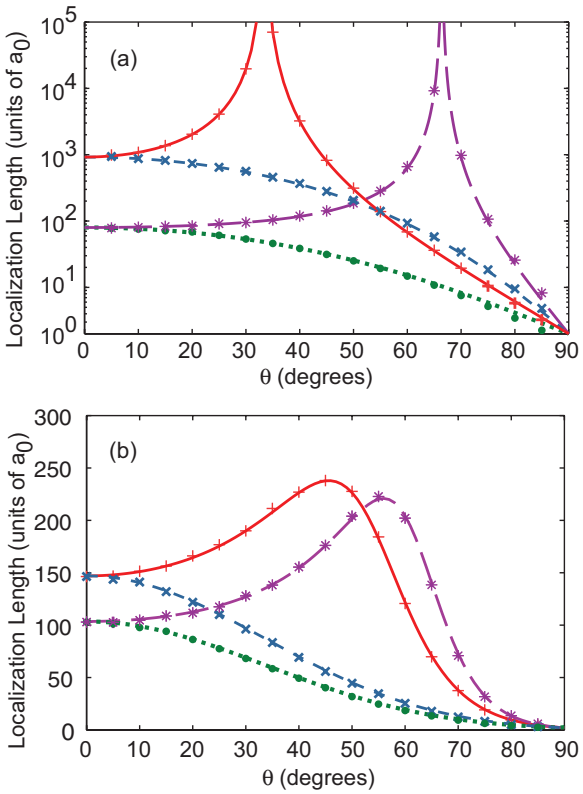

FIG. 2. (Color online) Angular dependence of $\xi_{s,p}$ (in units of a_0) for $n_a = 1.83, n_b = 1.46, n_0 = 1.33$. (a) Binary stacks ($f = 0,1$) and logarithmic scale. (b) Mixed stacks ($f = 0.5,0.75$) and linear scale. The weak scattering approximations are indicated by the continuous curves and the transfer matrix simulations are indicated by the discrete symbols. Red solid curves and cardinal crosses, p-polarization for $f = 0$ in (a) and $f = 0.5$ in (b); blue short-dashed curves and oblique crosses, s-polarization for $f = 0$ in (a) and $f = 0.5$ in (b); purple long-dashed curves and asterisks, p-polarization for $f = 1$ in (a) and $f = 0.75$ in (b); green dotted curves and solid circles, s-polarization for $f = 1$ in (a) and $f = 0.75$ in (b). The simulations were averaged over 10^3 stack configurations and for $\lambda = a_0$.

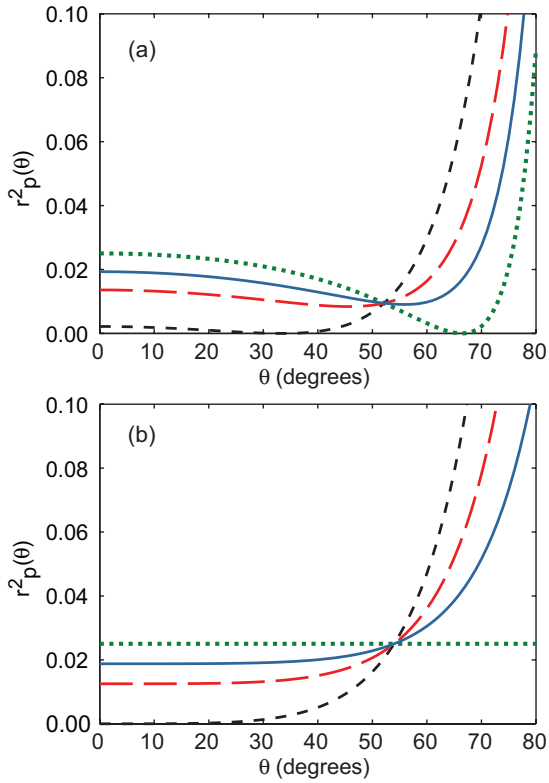

FIG. 3. (Color online) p-polarization reflection coefficients for: (a) $n_a = 1.83$, $n_b = 1.46$, $n_0 = 1.33$ (corresponding to Fig. 2); (b) $n_a = 1.83, n_b = 1.33, n_0 = 1.33$ (corresponding to Fig. 4). Black short-dashed curves: isotropic-positive uniaxial interface; green dotted curves: isotropic-negative uniaxial interfaces; red long-dashed curves: $f = 0.5$; blue solid curves: $f = 0.75$.

The angular dependence of $\xi_{s,p}$ for mixed stacks with both types of birefringent layer present is shown in Fig. 2(b) for $f = 0.5$, $f = 0.75$ and the same set of refractive index values as Fig. 2(a). It is clear that the maximum values of the ξ_p curves are of similar magnitude to the values at normal incidence. This is in contrast to isotropic stacks with fluctuating refractive indices where the localization length maxima are always at least 2 orders of magnitude greater than at normal incidence (as confirmed by both simulation[6] and mathematical analysis[11]). Again, due to the agreement between the weak scattering approximation (7) and the simulations, this can be readily explained through the properties of the p-polarization reflection coefficients [(10), Fig. 3(a)]. It is also apparent from Figs. 2(b) and 3(a) that it is possible to control the angular position of the maxima of ξ_p by using different values of f. It is important to emphasize that our particular set of refractive index values are not important for this form of behavior to occur. Qualitatively similar effects are observed whenever the birefringence $(n_a - n_b)$ is of the order of the planar interlayer refractive index difference $(n_{i,x} - n_0)$ and the angular separation between interfacial Brewster angles, (11), is sufficiently great ($\sim 25^\circ$ or more).

For the limiting "index-matching" case of our model where $n_b = n_0$, the p-polarization reflection coefficient for the isotropic-negative uniaxial layers is constant with angle of incidence. We would therefore predict that for $f = 1$, ξ_p should be constant at all angles of incidence and equal to $2a_0(n_a + n_0)^2/(n_a - n_0)^2$, from (7) and (10). However, an unusual delocalization effect occurs for the numerically exact transfer matrix simulations at large angles of incidence [Fig. 4(a)]. A physical argument for the origin of this behavior can be reached by considering the refraction angle for the p-polarization in the birefringent layers in the structure. As the p-polarization refractive index

$$n_p = \frac{n_a n_b}{\sqrt{n_a^2 \sin^2(\theta) + n_b^2 \cos^2(\theta)}} \tag{12}$$

$\to n_0$ for $n_b = n_0$ and $\theta \to 90^\circ$, the mean-free path between scattering events in the stack $\to \infty$ as $\theta \to 90^\circ$. Consequently the mixing between stationary states required in system that is necessary for localization is inhibited. It is important to note that this delocalization effect is a particular peculiarity of our index-matching alternating isotropic-birefringent stack system, and in general does not occur where there is a p-polarization refractive index contrast at $\theta = 90^\circ$. We do

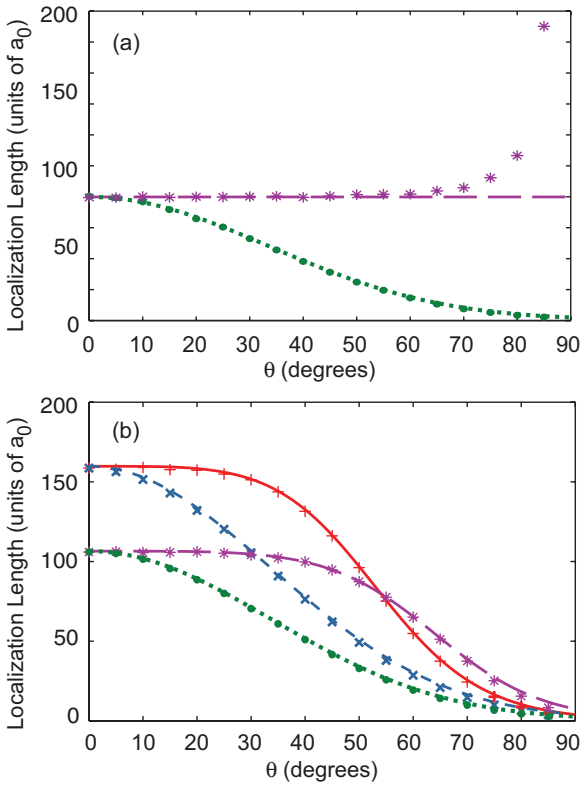

FIG. 4. (Color online) Angular dependence of $\xi_{s,p}$ (in units of a_0) for $n_a = 1.83$, $n_b = 1.33$, $n_0 = 1.33$: (a) binary stack ($f = 1$), (b) mixed stacks ($f = 0.5,0.75$). The weak scattering approximations are indicated by the continuous curves and the simulations are indicated by the discrete symbols. Purple long-dashed curves and asterisks: p-polarization for $f = 1$ in (a) and $f = 0.75$ in (b); green dotted curves and solid circles: s-polarization for $f = 1$ in (a) and $f = 0.75$ in (b); red solid curves and cardinal crosses, p-polarization for $f = 0.5$ in (b); blue dotted curves and oblique crosses: s-polarization for $f = 0.5$ in (b). The simulations were averaged over 10^3 stack configurations and for $\lambda = a_0$.

not show the more trivial case for $f = 0$ stacks, which have divergent ξ_p at $\theta = 0$ and infinite ξ_s at all angles of incidence.

For mixed index-matching structures there is an excellent agreement between the transfer matrix simulations and the weak scattering approximation over all angles of incidence [Fig. 4(b)]. Due to the positive uniaxial layers having $n_p = n_a$ for $\theta = 90^\circ$ from (12), localization is no longer inhibited as $\theta \to 90^\circ$. These mixed index-matching stacks have the unusual property that ξ_p is finite and monotonically decreases with angle of incidence, and is an effect that can be readily understood from the averaging of the index-matching interfacial reflection coefficients [Fig. 3(b)].

Our mixed stack system provides a generic means to effectively localize both s- and p-polarized light over all angles of incidence in random layered dielectric medium. This includes a complete suppression (in the sense that, in a similar fashion to ξ_s, ξ_p monotonically decreases with angle) of the Brewster anomaly effect. We should highlight here that no critical angle screening is required for this to occur and that, for our model of uncorrelated thickness disorder, the engineering of the properties of the localization length can be achieved simply through the averaging of the interfacial reflection coefficients in the stack. It has often been remarked that Brewster delocalization anomalies can only occur due to the higher dimensional, vectorial nature of electromagnetic waves (e.g., Refs. 10 and 11), and the problem therefore not being a purely 1D system. Perhaps it is only natural that another higher dimensional property, birefringence, can be exploited to reverse this anomalous behavior and effectively localize all the stationary states in the system.

To the best of our knowledge our study is the first time that the polarization dependence of localization length has been assessed in layered systems that include birefringence. We anticipate that our study will stimulate analysis of birefringent systems that have weak disorder and a wavelength dependance to their localization length, including further examples of biophotonic structures. Given the general robustness of Brewster anomaly effects in dielectric media with a range of weak and strong disorder,[6–12] we expect that the Brewster anomaly suppressing effects could also be achieved for many different forms of thickness disorder. In turn, this could then inform the design process of a new class of polarization-insensitive mirror based upon the averaging of the interfacial reflection coefficients in the structure. These devices would provide an alternative mechanism to produce nonpolarizing reflections, in addition to periodic omnidirectional mirrors which require critical angle screening.[27] While practical mirrors based upon localization properties only correspond to a single realization of a statistical ensemble, unbroken high reflection regions are none-the-less likely to be achievable for sufficiently thick structures.[14,15] A suitable class of materials with the necessary high birefringence required for such a disordered isotropic-birefringent mirror is high refractive index polymers.[28]

As a final comment, both disorder[29,30] and birefringence[17,19,31] are remarkably common properties of biological photonic structures. However, despite the fact that localization is fundamental to our understanding of the way that waves behave in random media, no studies have as yet explicitly investigated localization of light in a biological system. While the suppression of Brewster delocalization anomalies explains the key physics that underlies the mechanism of weakly polarizing reflections from silvery fish,[17] we envisage that the mathematical framework as set out above provides the necessary foundation for future investigations into the localization of light in biological structures that include both weak structural disorder and birefringent layers. Revisiting such structures within the context of localization could provide great insight for the theoretical study of how complex optical systems use disorder and birefringence to enhance desirable optical properties.

The authors acknowledge support from the Biotechnology and Biological Sciences Research Council (N.W.R., Grant No. BB/G022917/1; N.W.R. and J.C.P., Grant No. BB/H01635X/1), the Engineering and Physical Sciences Research Council (T.M.J., Grant No. EP/E501214/1), and the Air Force Office of Scientific Research (N.W.R., Grant No. FA8655-12-1-2112). The authors thank M. V. Berry, J. P. Keating, and M. R. Dennis for helpful discussions.

*nicholas.roberts@bristol.ac.uk

[1]P. W. Anderson, Phys. Rev. Lett. **109**, 1492 (1958).
[2]S. John, Phys. Rev. Lett. **53**, 2169 (1984).
[3]S. John, Phys. Today **44**(5), 32 (1991).
[4]N. F. Mott and W. D. Twose, Adv. Phys. **10**, 107 (1961).
[5]H. Furstenberg and L. Xy, Trans. Am. Math. Soc. **168**, 377 (1962).
[6]J. E. Sipe, P. Sheng, B. White, and M. Cohen, Phys. Rev. Lett. **60**, 108 (1988).
[7]A. Aronov and V. Gasparin, Solid State Commun. **73**, 61 (1990).
[8]A. Aronov, V. Gasparin, and U. Gummich, J. Phys.: Condens. Matter **3**, 3023 (1991).
[9]X. Du, D. Zhang, X. Zhang, B. Feng, and D. Zhang, Phys. Rev. B **56**, 28 (1997).
[10]K. Yu Bliokh and V. D. Freilikher, Phys. Rev. B **70**, 245121 (2004).
[11]Ara A. Asatryan, L. C. Botten, M. A. Byrne, V. D. Freilikher, S. A. Gredeskul, I. V. Shadrivov, R. C. McPhedran, and Y. S. Kivshar, Phys. Rev. B **82**, 205124 (2010).
[12]K. J. Lee and K. Kim, Opt. Express **19**, 570 (2011).
[13]M. Berry and S. Klein, Eur. J. Phys. **18**, 222 (1997).
[14]D. Zhang, Z. Li, W. Hu, and B. Cheng, Appl. Phys. Lett. **67**, 2431 (1995).
[15]H. Li, H. Chen, and X. Qiu, Physica B: Condensed Matter **279**, 164 (2000).
[16]Y. Fink, J. N. Winn, S. Fan, C. Chen, M. Jurgen, J. D. Joannopoulos, and E. L. Thomas, Science **282**, 1679 (1998).
[17]T. M. Jordan, J. C. Partridge, and N. W. Roberts, Nat. Photonics **6**, 759 (2012).
[18]P. Vukusic and R. J. Sambles, Nature (London) **424**, 852 (2003).
[19]N. W. Roberts, T. H. Chiou, N. J. Marshall, and T. W. Cronin, Nat. Photonics **3**, 641 (2009).
[20]Y.-J. Jen, A. Lakhtakia, C.-W. Yu, C.-F. Lin, M.-J. Lin, S.-H. Wang, and J.-R. Lai, Nat. Commun. **2**, 363 (2011).
[21]D. Berreman, J. Opt. Soc. Am. **62**, 502 (1972).
[22]R. M. Azzam and N. M. Bashara, *Ellipsometry and Polarized Light* (Elsevier, 1988), pp. 269–363.
[23]S. A. Gredeskul, Y. S. Kivshar, A. A. Asatryan, K. Y. Bliokh, Y. P. Bliokh, V. D. Freilikher, and I. V. Shadrivov, J. Low Temp. Phys. **38**, 570 (2012).
[24]I. M. Lifshitz, S. A. Gredeskul, and L. Pastur, *Introduction to the Theory of Disordered Systems* (Wiley, New York, 1989).
[25]S. Orfanidis, *Electromagnetic Waves and Antennas* (online; accessed March 28, 2013; http://www.ece.rutgers.edu/∼orfanidi/ewa).
[26]E. J. Denton, Philos. Trans. R. Soc. B: Biological Sciences **258**, 285 (1970).
[27]J. N. Winn, Y. Fink, S. Fan, and J. D. Joannopoulos, Opt. Lett. **23**, 1573 (1998).
[28]M. F. Weber, C. Stover, L. Gilbert, T. Nevitt, and A. Ouderkirk, Science **287**, 2451 (2000).
[29]E. J. Denton and M. F. Land, Proc. R. Soc. London B **178**, 43 (1971).
[30]A. Holt, A. M. Sweeney, S. Johnsen, and D. E. Morse, Proc. R. Soc.: Interface **8**, 1386 (2011).
[31]H.-J. Wagner, R. H. Douglas, T. M. Frank, N. W. Roberts, and J. C. Partridge, Curr. Biol. **19**, 108 (2009).